**SUPPLEMENTARY INFORMATION ACCOMPANYING**

# PROTOCADHERINS MEDIATE DENDRITIC SELF-AVOIDANCE IN THE MAMMALIAN NERVOUS SYSTEM

Julie L. Lefebvre[1], Dimitar Kostadinov[1], Weisheng V. Chen[2], Tom Maniatis[2], Joshua R. Sanes[1]*

[1]Center for Brain Science and Department of Molecular and Cellular Biology, Harvard University, 52 Oxford Street, Cambridge, MA 02138

[2]Department of Biochemistry and Molecular Biophysics, Columbia University Medical Center, 701 W 168th Street, New York, NY 10032

CONTENTS:

Supplementary Figure 1

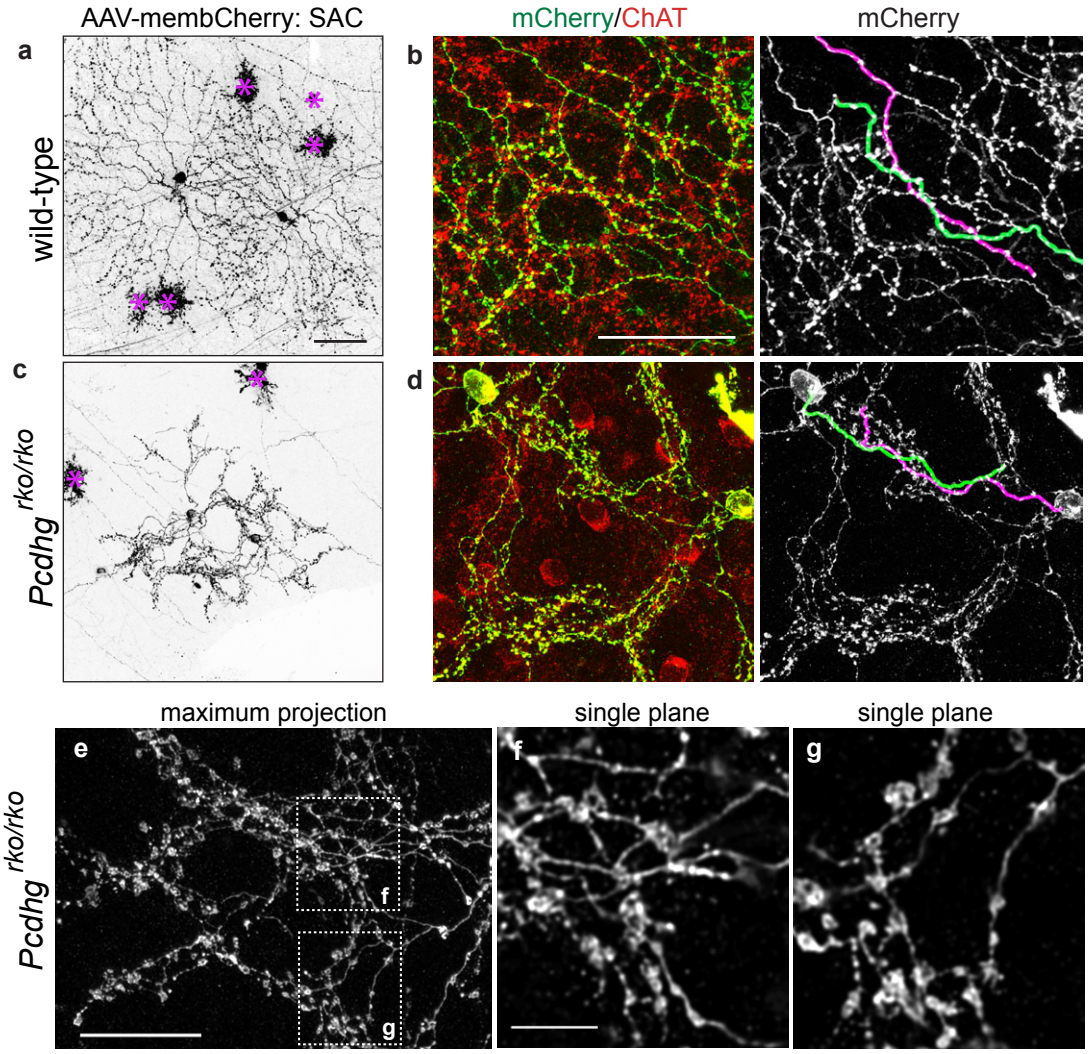


**Figure S1. Heteroneuronal association between neighboring SAC dendrites.**

**a,** Dendrites of two labeled neighboring SACs that overlap extensively in wild-type retina.

**b,** Distal dendrites of two labeled SACs (green) freely overlap and associate with the ChAT-labeled SAC plexus (red). Right panel, tracing of single distal dendrites arising from 2 SACs (green for one and magenta for the other) demonstrates overlap between heteroneuronal dendrites.

**c,d,** As in **a,b**, but in mutant *Pcdhg*$^{rko/rko}$ retina.

**e-g,** Images acquired at Nyquist limit resolution by oversampling and processing by deconvolution (see Online Methods for software) show crossings of *Pcdhg*$^{rko/rko}$ SAC dendrites in single optical sections.

Scale bars, 50 µm in **a-d**, 20 µm in **e**, and 5 µm in **f,g**.

* Asterisks denote non-SAC labeled neurons.

# Supplementary Figure 2

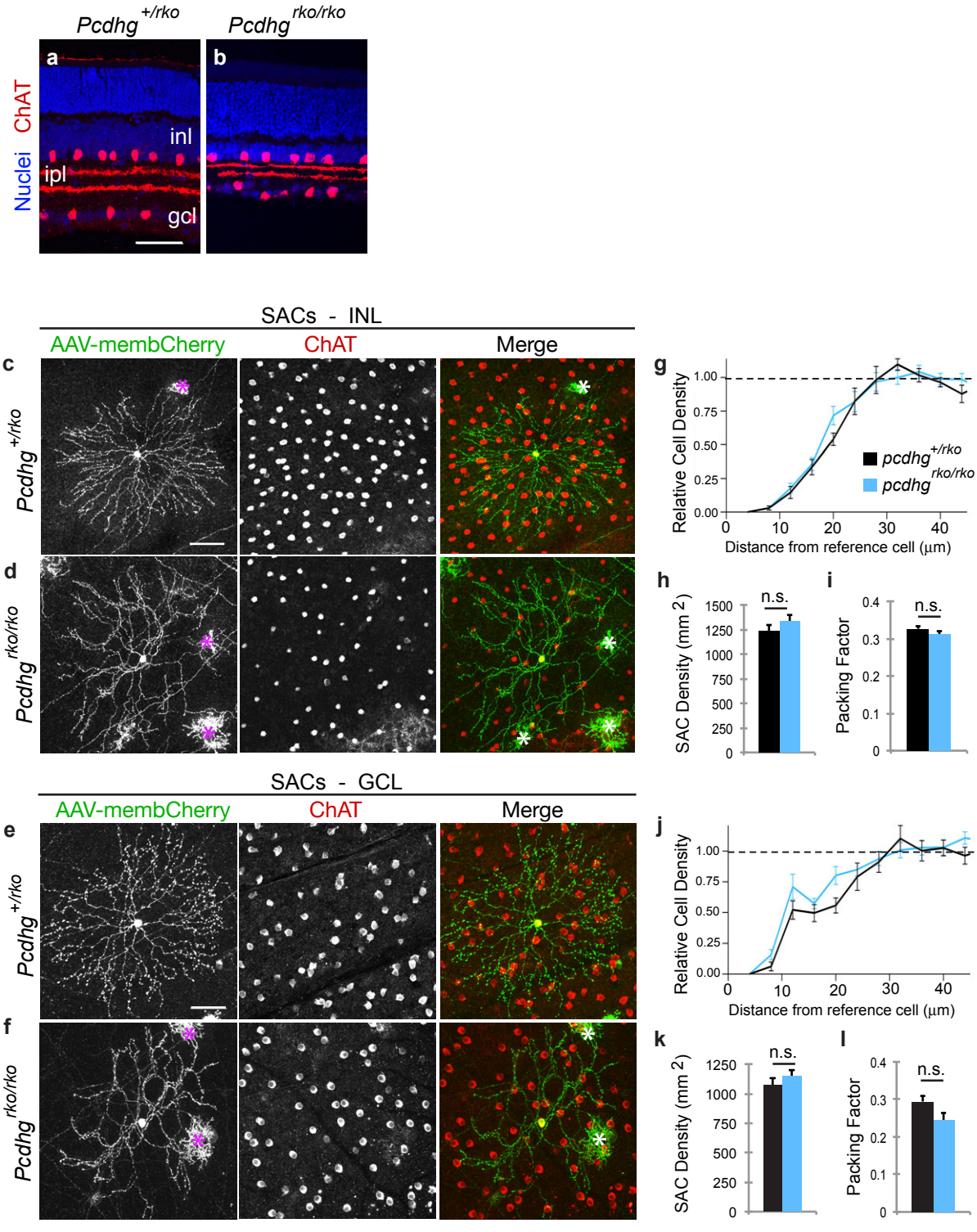

**Figure S2. Laminar targeting, density, and mosaic arrangement of SACs are unaffected in the absence of Pcdhgs.**

**a,b,** Cross-section of wild-type and *Pcdhg*$^{rko/rko}$ retina labeled with nuclear marker Popro1 and SAC marker ChAT. ChAT-positive SAC somata reside in INL (inner nuclear layer) and GCL (ganglion cell layer) and processes target and ramify in appropriate sublaminae in control (**a**) and in mutant *Pcdhg*$^{rko/rko}$ retina (**b**). Reduced INL and IPL in mutant are due to elevated loss of interneurons and RGCs (see ref. 22).

**c-f,** In the INL and GCL, SACs stained with ChAT reveal mosaic arrangements of SAC somata in flatmount preparations of wild-type and *Pcdhg*$^{rko/rko}$ mutant retinas. Scale bars, 50 μm.

**g,** Mosaic spacing of SAC arrays in INL as measured by Density recovery profiles (DRPs). DRP graph shows the density of somata present in a ring of radius *x* from each cell. Dashed line is mean density for whole image and represents a random distribution. Mosaic spacing is marked by an exclusion zone, which is represented here as the distance between the observed and random distributions. DRPs do not differ between wild-type (black) and mutants (blue).

**h,i,** SAC density and packing factor (a regularity index ranging between 0 [a randomly-distributed array] and 1 [a perfect hexagonal array]) in INL in mutants were indistinguishable from wild-type.

**j-l,** SAC DRPs (**j**), density (**k**) and packing factor (**l**) in GCL did not differ between mutants (blue) and wild-type (black). n.s., not significant, by Student's *t* test. All data are mean ± s.e.m. WT, n=9 from 2 animals; mutant, n =14, 4 animals.

Supplementary Figure 3

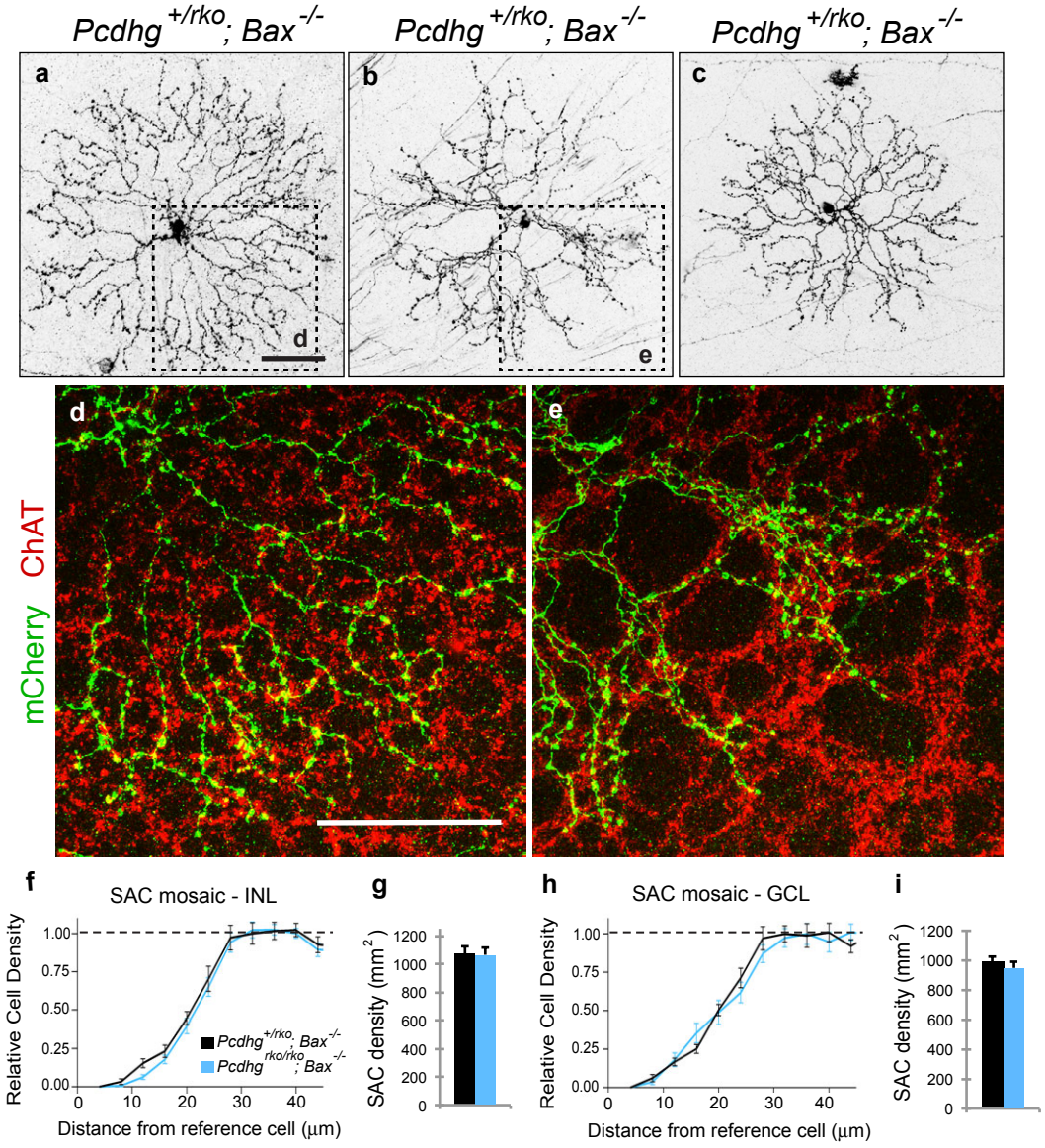


**Figure S3. Self-avoidance defects persist in Pcdhg mutant SACs following genetic blockade of programmed cell death.**

**a-c**, Morphology of SACs in *Bax*$^{-/-}$ and *Pcdhg* $^{rko/rko}$*; Bax*$^{-/-}$ double mutant retinas. Self-crossing and bundling defects of SAC dendrites are present in *Pcdhg* $^{rko/rko}$*; Bax*$^{-/-}$ double mutants.

**d,e,** Higher magnification of SAC dendrite morphology of insets in wild-type (**a**) and mutant (**b**). Labeled dendrites (green) are confined to ChAT-labeled SAC plexus (red), and show dramatic crossings in double mutants. Scale bars, 50 µm.

**f-i,** Mosaic spacing and density of SACs in INL and GCL are indistinguishable in *Bax*$^{-/-}$ and *Pcdhg* $^{rko/rko}$*; Bax*$^{-/-}$ double mutant retinas. DRP analysis as in Supplementary Figure 2. n ≥12 from 3-4 animals per genotype.

Supplementary Figure 4

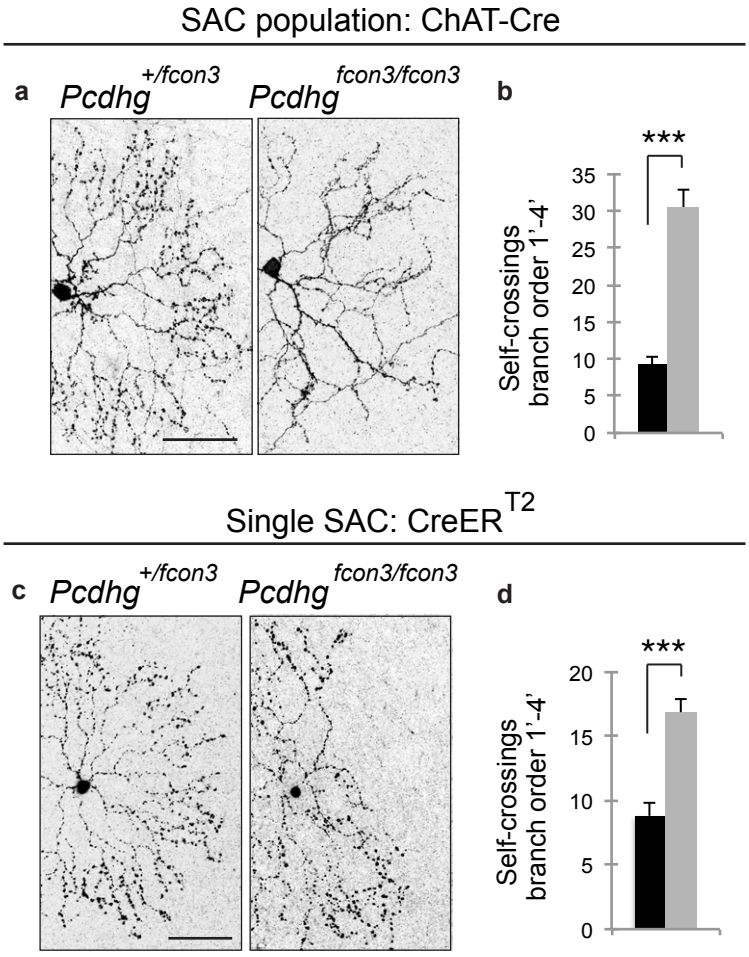


**Figure S4. Selective removal of Pcdhgs in SAC population and in single SACs disrupts dendrite self-avoidance.**

**a-d,** SAC self-avoidance defects are present following selective Pcdhg inactivation in SACs using ChAT-Cre (**a**, right panel) or in single mutant SACs generated by tamoxifen-activation of CreER (**c**, right panel). SACs were labeled with AAV in **a** and with a Cre-responsive reporter in **c**.

**b,d,** show increased self-crossings in 1st-4th order dendrites of mutant SACs (gray; n = 9 in **b** and n=20 in **d**) compared to controls (black; n=9, 11). Bars are mean ± s.e.m., *** *P<0.001.*

Scale bars, 50 μm.

Supplementary Figure 5

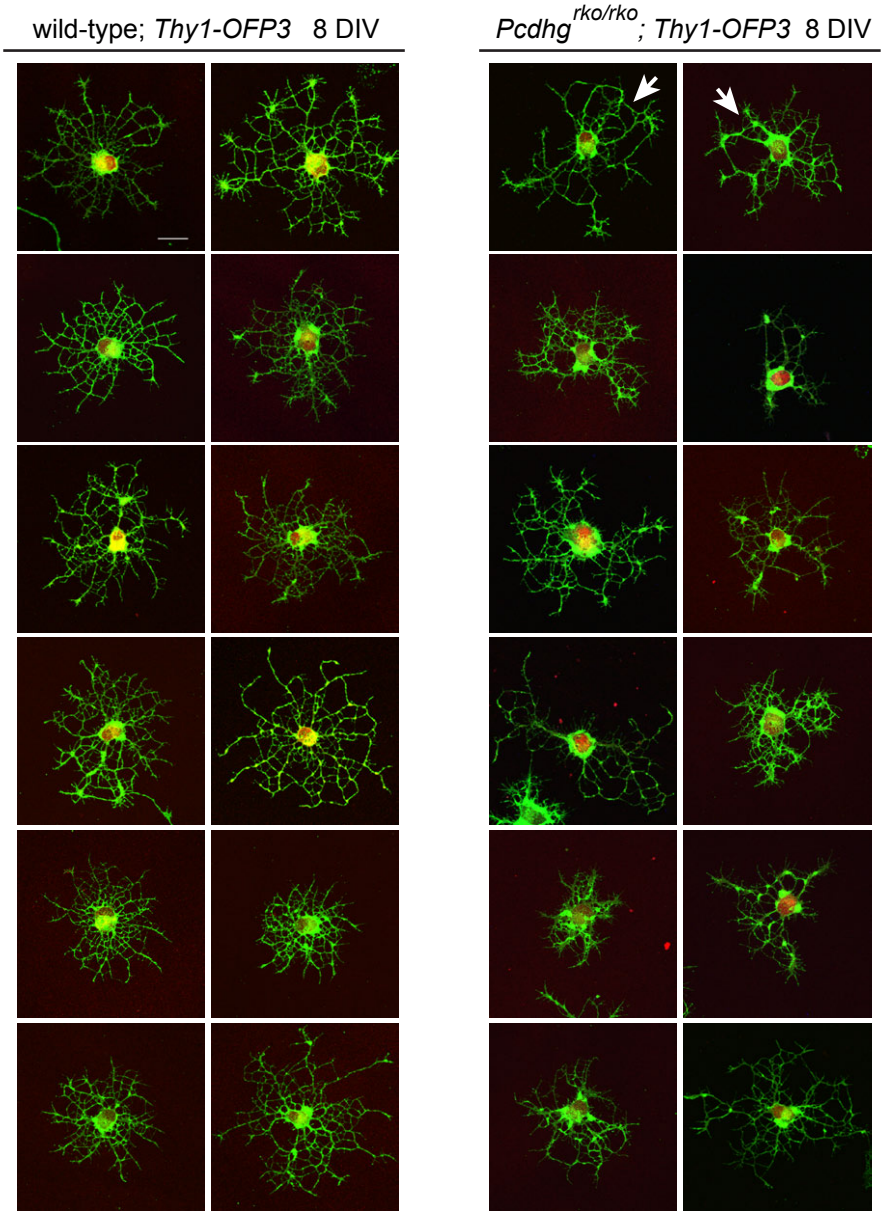


**Figure S5. Isolated SACs cultured in vitro show outgrowth defects.**

OFP+ SACs from dissociated retinas of Thy1-OFP3 transgenic P2 animals were isolated by FACS and cultured in vitro for 8 days. Isolated SACs are marked by OFP (red) and immunostained with syntaxin (green). Compared to the radial, web-like array of neurites of wild-type SACs (gallery on left), *Pcdhg* mutant SACs exhibit neurite outgrowth defects such as bundling (arrows) and loss of symmetric outgrowth (gallery on right).
Scale bar, 20 μm.

Supplementary Figure 6

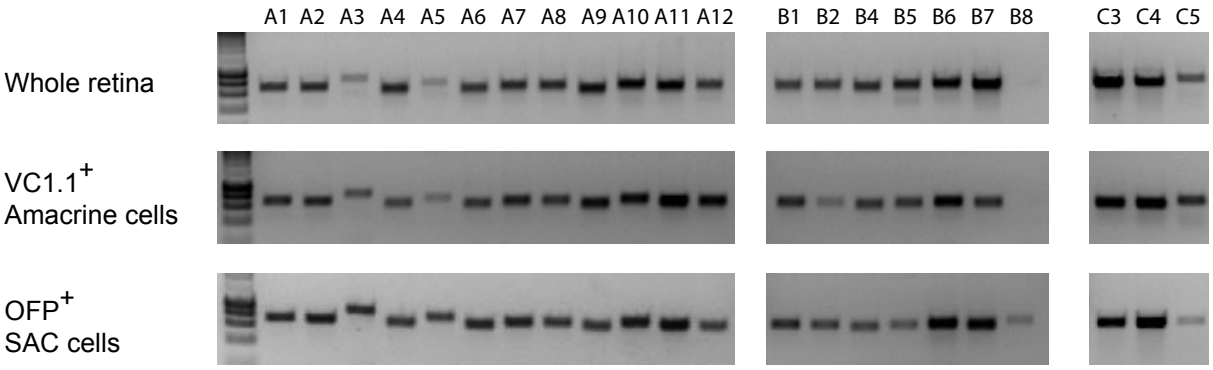


**Figure S6. All 22 Pcdhg variable transcripts are expressed by SACs.**

Expression profile of 22 Pcdhg variable transcripts by RT-PCR using isoform-specific primers. Whole retina, amacrine cells sorted by VC1.1+ expression, and OFP+ sorted SACs were isolated and profiled by RT-PCR. Purity of the sorted populations were confirmed by showing that markers of other cell types (*brn3a* and *brn3b* for RGCs, *trpm1* and *grm6* for bipolar cells, *rho* for rods) were expressed by whole retina but not SACs, whereas *chat* was expressed at many-fold higher levels by SACs than by whole retina (data not shown).

# Supplementary Figure 7

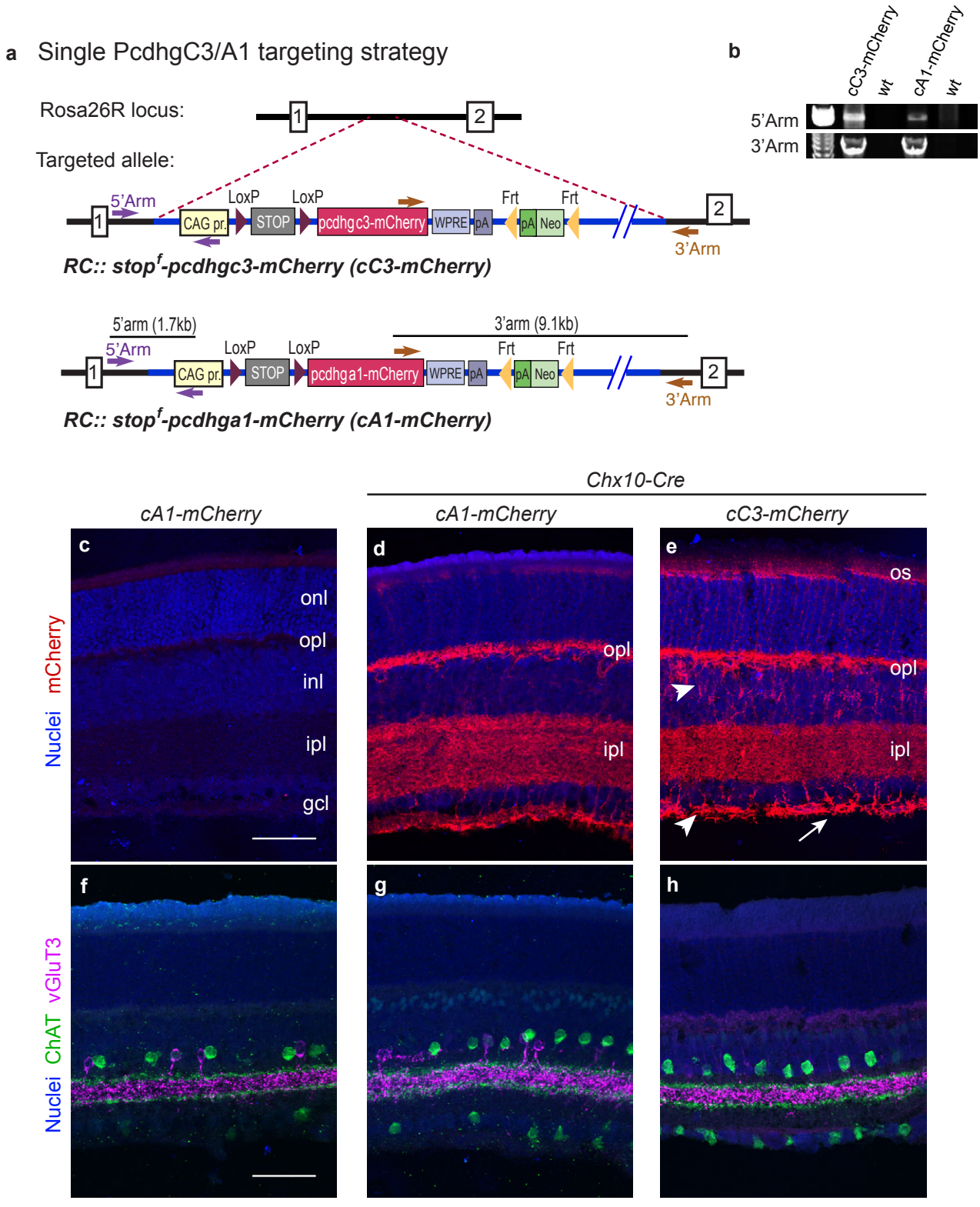

**Figure S7. Single Pcdhg isoform 'rescue' strategy.**

**a,** Diagram of targeting strategy to insert a cassette encoding *Pcdhga1* or *Pcdhgc3* cDNA fused to mCherry at the C'terminus into the Rosa26 locus, between exons 1 and 2. See Online Methods and ref.40 for more details. Targeting construct also includes a CAG promoter (chicken β-actin promoter and CMV immediate-early enhancer), a LoxP flanked 'Stop'[41], WPRE (woodchuck posttranslational response element)[36], polyadenylation signal (pA), and a *Frt*-flanked Neomycin selection cassette. Arrows show location of primers used for genotyping.

**b,** Validation of *cC3- and cA1-mCherry* targeting by PCR from genomic DNA.

**c-e,** Cre-dependent expression and appropriate localization of PcdhgA1-mCherry and PcdhgC3-mCherry fusion proteins was confirmed by immunostaining of retina cross-sections with antibody against mCherry (red). In the absence of Cre, no mCherry was detected (**c**). With Chx10-Cre activity, PcdhgA1-mCherry and PcdhgC3-mCherry fusion proteins were present in the synaptic OPL and IPL, as well as in outer segment (os), Muller glia processes and endfeet (arrowheads) and RGC axonal layer (arrow). Overexpression of a Pcdhg isoform in wild-type retina does not disrupt laminar organization of cellular (blue) and synaptic layers.

**f-h,** Processes of ChAT-labeled SAC (green) and vGluT3-positive amacrine subsets (magenta) target appropriate sublaminae in IPL in wild-type retina overexpressing PcdhgA1-mCherry (**g**) or PcdhgC3-mCherry (**h**).

Scale bars, 50 μm.

Supplementary Figure 8

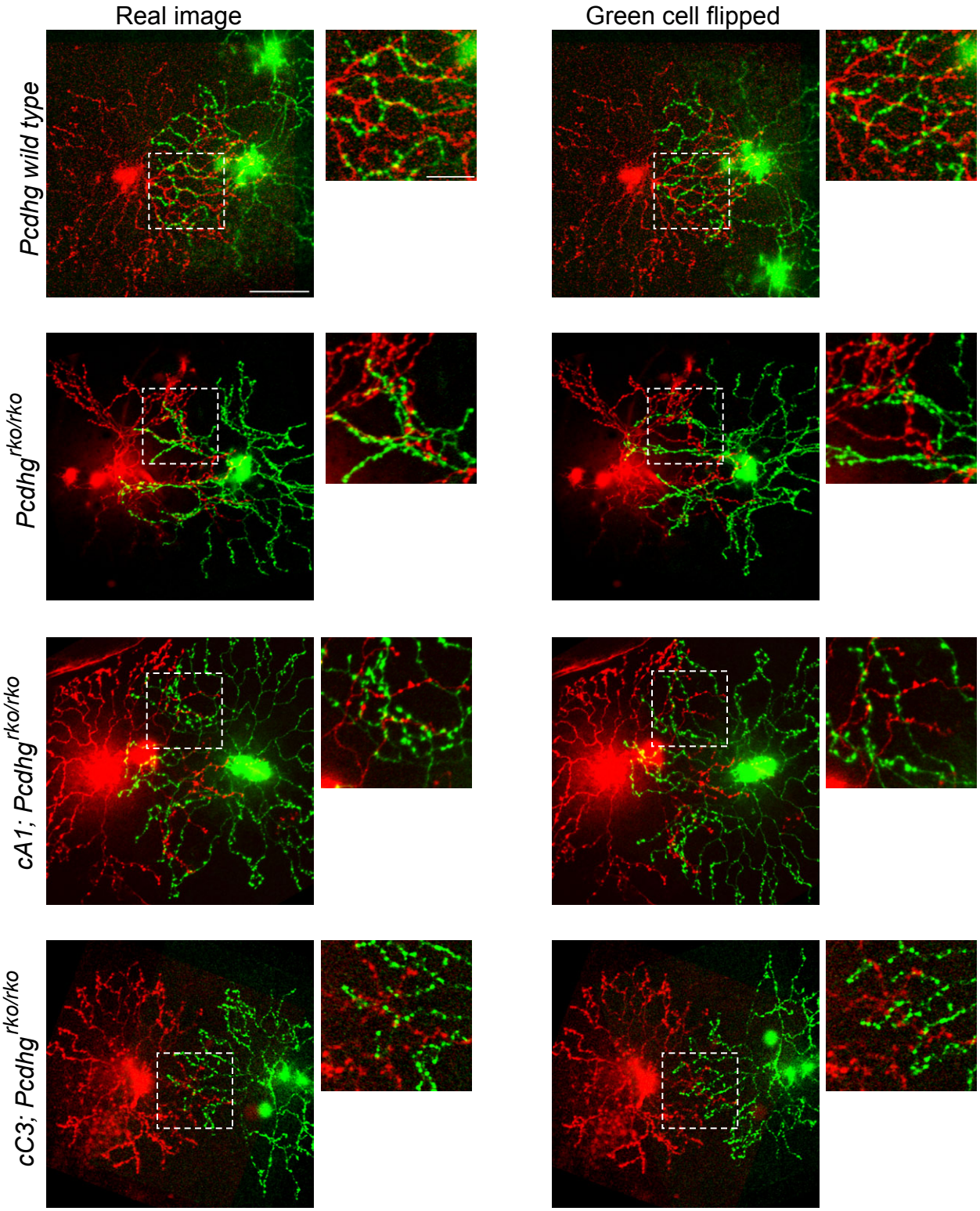

**Figure S8. Requirement of *Pcdhg* diversity on heteroneuronal interactions of SACs.**

Two nearby SACs from mice of indicated genotypes were injected with contrasting fluorescent dyes. Magnifications of boxed insets of full sized images are shown right to the right of each image. The left column of images shows the real images of paired SAC fills. The right shows the same images, with the green cell digitally flipped and realigned to the center of the cell bodies. Quantitative data from these and other pairs are shown in Fig. 4f,g.
Scale bars, 50 μm for full sized images and 20 μm for insets.

Supplementary Figure 9

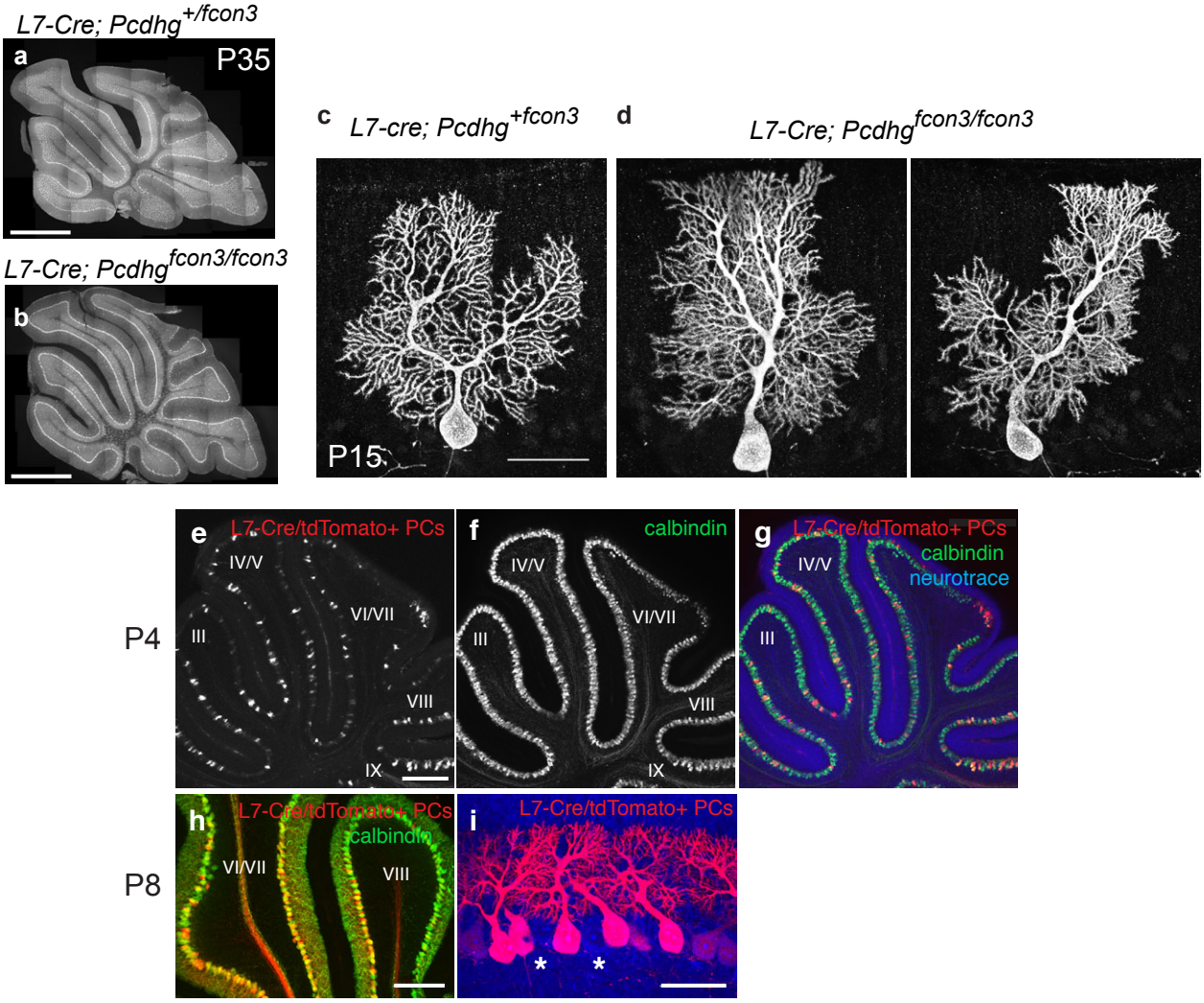


**Figure S9. L7/Pcp2-Bac::Cre recombination pattern in the developing cerebellum.**

**a,b,** Cross sections of control and *L7-cre; Pcdhg*$^{fcon3/fcon3}$ mice showing that overall cerebellar size is unchanged in the mutant. Because the size (here) and Purkinje cell number per unit length (Figure 5i) do not differ between mutants and controls, we believe that total Purkinje cell number is unaffected by Pcdhg deletion.

**c,d,** Dendrite self-crossing and disorganization is detected in developing PC arbor in Pcdhg mutants at P15.

**e-i,** Sagittal brain sections of L7-Cre; RC-Stopflox-tdTomato mice illustrate L7/Pcp2-Cre mediated recombination pattern marked by expression of td-Tomato in recombined Purkinje cells (red). Purkinje cells (PC) are labeled with anti-Calbindin (green) and nuclei with Neurotrace (blue). By P4, there are very sparse recombined PCs throughout the cerebellum, with increased numbers in the posterior lobules VII-IX (**e**).By P8, the number of recombined PCs (red) increases (**h,i**), but unrecombined cells are still present (asterisks) in **i**.

Scale bars, 1mm in **a,b**; 50 μm in **c,d** and **i**, and 200 μm in **e-h**.

**Supplementary Table 1: PCR primers for RT-PCR analysis**

| Primer Target/Name | Amplicon size | Primer sequence (5'-3') |
|---|---|---|
| **Pcdhga1-F** | **669** | **CTTGGTGCTCAAGCTGCGACA** |
| **Pcdhga2-F** | **658** | **GCTGAGGCGCTGGCATCTGT** |
| **Pcdhga3-F** | **795** | **CTGGGGGACCTGGAAAGCATC** |
| Pcdhga4-F | 612 | TGGGTTGTCATCCTTGCCTG |
| **Pcdhga5-F** | **622** | **CCACAGGCAGATTGGCCGAC** |
| Pcdhga6-F | 600 | GTCCACTTCACATTTCGTGG |
| Pcdhga7-F | 628 | GCTACAGGCTTCTTCAGGTG |
| **Pcdhga8-F** | **628** | **CCAGCTCCAGGGCTCCAGAA** |
| **Pcdhga9-F** | **584** | **GTGGGTGTGCATGGGGTTCAGA** |
| **Pcdhga10-F** | **654** | **GCGCTGGCACAAGTCTCACG** |
| **Pcdhga11-F** | **618** | **ATTGGCTGGTGTGCCTCCTTCG** |
| Pcdhga12-F | 603 | CGTTGCAGCCTCTCACTTTG |
| Pcdhgb1-F | 594 | CCTGAAGTCTCAACCTGTGG |
| Pcdhgb2-F | 592 | CTCTAACCTTGCGACTGGAG |
| Pcdhgb4-F | 566 | GCTTTCAGTCGGAAGTGGTG |
| Pcdhgb5-F | 588 | TCTAAGCCTGTGGTTTTCCC |
| **Pcdhgb6-F** | **618** | **TCAGTCTGGTCTTTGTTCTAAGGCT** |
| Pcdhgb7-F | 590 | CTAGACCAGTACTTCCACCC |
| **Pcdhgb8-F** | **663** | **CCTTCGCCTTCGACAGTCCC** |
| Pcdhgc3-F | 612 | GTGAGCTCCCTGTACCGAAC |
| Pcdhgc4-F | 614 | TCACCAGATCTCGGAGGAGG |
| **Pcdhgc5-F** | **649** | **GCAGGGGCCAGGACTCACC** |
| **Pcdhg-conex3R** | | **CCATATTACTTCTTCTCTTTCTTGCCC** |
| | | **bold** = modified from ref. 21. |
| ChAT-F<br>ChAT-R<br>(SAC marker) | 634 | CTGGCAACTTCGTCGGAGGC<br>TGGCTGTCCAGCAGAGCCTT |
| Brn3a-F<br>Brn3a-R<br>(RGC marker) | 618 | ATCTGCGACTCGGACACGGA<br>CATGGGACTCCTGCCCCCAA |
| Brn3b-F<br>Brn3b-R<br>(RGC marker) | 613 | TAGCGGGAGACACAGGAGCG<br>GGTAAGTGGCGTCCGGCTTG |
| Gad1<br>(amacrine marker) | 102 | CTGTGACTCGCTTAGCTGAAACCT<br>GCACAGTGTGGGTTTCATGTCTTC |
| mGluR6-F<br>mGluR6-R<br>(bipolar marker) | 527 | CAAGGCCCGAGGTGTGCCAG<br>GGCCAGCCTGCCCAGGAAAG |
| Trpm1-F<br>Trpm1-R<br>(bipolar marker) | 367 | GCGTGGTTCAATCAAGAGCTC<br>CATGAGGTGGAGCAGGGAATCTG |
| Rhodopsin-F<br>Rhodopsin-R<br>(Rod photoreceptor marker) | 370 | CTACTTCGTCTTTGGGCCCACAG<br>CCCATAGCAGAAGAAGATGACGATCA |
| Beta-actin-F<br>Beta-actin-R | 168 | ACCAACTGGGACGACATGGAGAA<br>CATGGCTGGGGTGTTGAAGGT |
| | | |